

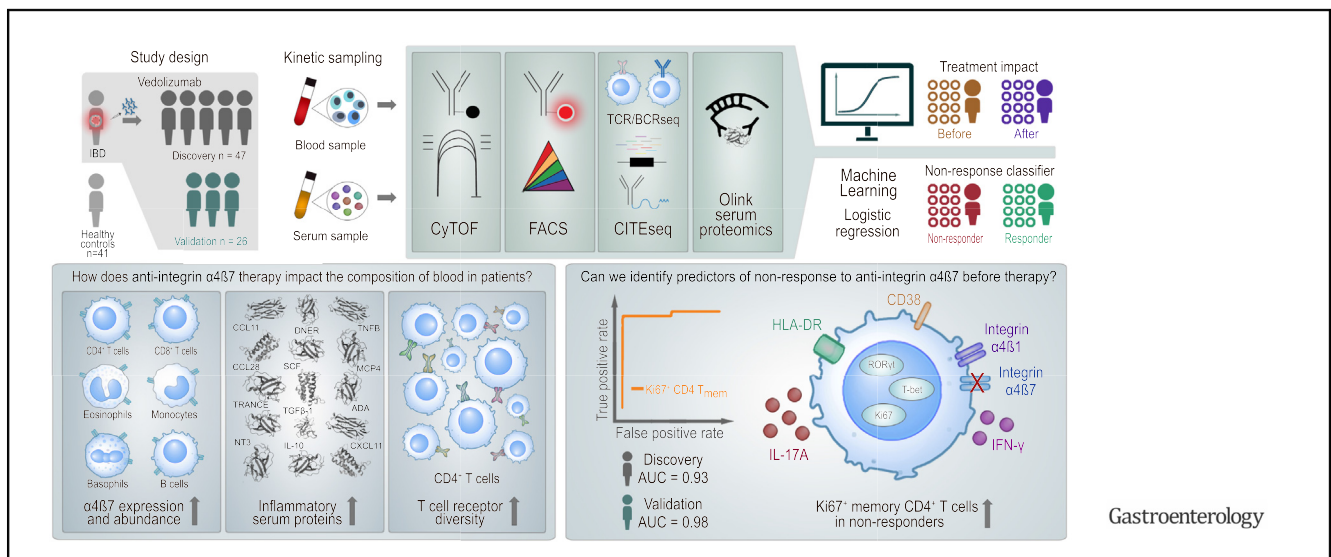
INFLAMMATORY BOWEL DISEASE

Multimodal Profiling of Peripheral Blood Identifies Proliferating Circulating Effector CD4⁺ T Cells as Predictors for Response to Integrin $\alpha4\beta7$ -Blocking Therapy in Inflammatory Bowel Disease



Veronika Horn,^{1,2,*} Camila A. Cancino,^{1,2,*} Lisa M. Steinheuer,^{3,*} Benedikt Obermayer,^{4,*} Konstantin Fritz,^{1,2} Anke L. Nguyen,^{1,5} Kim Susan Juhran,^{1,2} Christina Plattner,⁶ Diana Bösel,^{1,2} Lotte Oldenburg,⁷ Marie Burns,² Axel Ronald Schulz,² Mariia Saliutina,^{1,2} Eleni Mantzivi,¹ Donata Lissner,¹ Thomas Conrad,^{8,9} Mir-Farzin Mashreghi,^{2,10} Sebastian Zundler,¹¹ Elena Sonnenberg,¹ Michael Schumann,¹ Lea-Maxie Haag,¹ Dieter Beule,⁴ Lukas Flatz,^{12,13} TRR241 IBDome Consortium, Zlatko Trajanoski,⁶ Geert D'Haens,⁷ Carl Weidinger,¹ Henrik E. Mei,² Britta Siegmund,¹ Kevin Thurley,^{2,3} and Ahmed N. Hegazy^{1,2,14}

¹Charité-Universitätsmedizin Berlin, corporate member of Freie Universität Berlin and Humboldt-Universität zu Berlin, Department of Gastroenterology, Infectious Diseases and Rheumatology, Berlin, Germany; ²Deutsches Rheuma-Forschungszentrum, ein Institut der Leibniz-Gemeinschaft, Berlin, Germany; ³Institute of Experimental Oncology, Biomathematics Division, University Hospital Bonn, Bonn, Germany; ⁴Berlin Institute of Health at Charité-Universitätsmedizin Berlin, Core Unit Bioinformatics, Berlin, Germany; ⁵Department of Gastroenterology, Central Clinical School, Monash University and Alfred Health, Melbourne, Victoria, Australia; ⁶Biocenter, Institute of Bioinformatics, Medical University of Innsbruck, Innsbruck, Austria; ⁷Department of Gastroenterology, Amsterdam University Medical Centers, Amsterdam, The Netherlands; ⁸Genomics Technology Platform, Max Delbrück Center for Molecular Medicine in the Helmholtz Association, Berlin, Germany; ⁹Core Unit Genomics, Berlin Institute of Health at Charité-Universitätsmedizin Berlin, Berlin, Germany; ¹⁰German Center for Child and Adolescent Health (DZKJ), Partner Site Berlin, Berlin, Germany; ¹¹Department of Medicine 1, University Hospital Erlangen and Friedrich-Alexander-Universität Erlangen-Nürnberg, Germany; ¹²Institute of Immunobiology, Kantonsspital St. Gallen, St. Gallen, Switzerland; ¹³Department of Dermatology, University Hospital Tübingen, University of Tübingen, Tübingen, Germany; and ¹⁴Berlin Institute of Health at Charité-Universitätsmedizin Berlin, Berlin Institute of Health Academy, Clinician Scientist Program, Berlin, Germany



BACKGROUND & AIMS: Despite the success of biological therapies in treating inflammatory bowel disease, managing patients remains challenging due to the absence of reliable predictors of therapy response. **METHODS:** In this study, we prospectively sampled 2 cohorts of patients with inflammatory bowel disease receiving the anti-integrin $\alpha4\beta7$ antibody vedolizumab. Samples were subjected to mass cytometry;

single-cell RNA sequencing; single-cell B and T cell receptor sequencing (BCR/TCR-seq); serum proteomics; and multiparametric flow cytometry to comprehensively assess vedolizumab-induced immunologic changes in the peripheral blood and their potential associations with treatment response. **RESULTS:** Vedolizumab treatment led to substantial alterations in the abundance of circulating immune cell

lineages and modified the T-cell receptor diversity of gut-homing CD4⁺ memory T cells. Through integration of multimodal parameters and machine learning, we identified a significant increase in proliferating CD4⁺ memory T cells among nonresponders before treatment compared with responders. This predictive T-cell signature demonstrated an activated T-helper 1/T-helper 17 cell phenotype and exhibited elevated levels of integrin $\alpha 4\beta 1$, potentially making these cells less susceptible to direct targeting by vedolizumab. **CONCLUSIONS:** These findings provide a reliable predictive classifier with significant implications for personalized inflammatory bowel disease management.

Keywords: Inflammatory Bowel Disease; Cell Migration and Homing; Integrin $\alpha 4\beta 7$; CD4⁺ Memory T Cells; Vedolizumab; Single-Cell Profiling; Machine Learning; Therapy Response.

Recent therapies for inflammatory bowel disease (IBD) target pathogenic cytokine pathways and immune cell recruitment to the gut.¹⁻⁴ Vedolizumab, a monoclonal antibody, selectively inhibits lymphocyte homing to the intestine by disrupting interactions between mucosal vascular addressin cell adhesion molecule-1 (MAdCAM-1) on gut endothelial cells and integrin $\alpha 4\beta 7$ on circulating leukocytes.⁵⁻⁸ Vedolizumab induces and maintains clinical remission in patients with Crohn's disease (CD) and ulcerative colitis (UC).⁹⁻¹¹ It is believed to act on gut-homing T-cell subsets, but recent reports have indicated effects on other cell types known to express integrin $\alpha 4\beta 7$, such as monocytes, eosinophils, and plasmablasts.¹¹⁻¹³ Integrin $\alpha 4\beta 7$ blockade increases total numbers of peripheral blood mononuclear cells (PBMCs) and circulating memory T cells, suggesting that it sequesters gut-homing cells in the blood, thereby reducing their numbers in the mucosa and gut-associated lymphoid tissue.^{12,14-17}

Despite this knowledge, only a fraction of patients respond to vedolizumab or experience full remission, underscoring the unmet need for a more comprehensive understanding of its mode of action and the factors and mechanisms behind treatment failure.^{9,10,18,19} In addition, identifying biomarkers or correlates of therapy failure could help to deploy specific biological therapies to patients with IBD who are more likely to respond.¹⁹⁻²¹ There have been attempts to identify potential predictors of therapy response to vedolizumab based on (para-)clinical parameters, such as C-reactive protein, interleukin (IL) 6/8, and integrin $\alpha 4\beta 7$ expression on circulating and lamina propria T cells, the composition of the fecal microbiota, and cellular and transcriptomic cues in the intestinal mucosa.²²⁻³⁰ However, none of these biomarkers are clinically established, and the immunologic correlates of anti-integrin treatment responsiveness, especially in peripheral blood, remain undefined.

In this prospective cohort study, we employed multimodal profiling to systematically evaluate the circulating immune landscape both at baseline and after vedolizumab treatment. We observed highly dynamic changes within the innate and adaptive immune cell compartments during

WHAT YOU NEED TO KNOW

BACKGROUND AND CONTEXT

Patients with inflammatory bowel disease (IBD) have benefitted from new biologic treatments, including the anti-integrin $\alpha 4\beta 7$ blocker vedolizumab. However, many patients do not achieve full remission and there are no reliable markers to predict responses.

NEW FINDINGS

The circulating immune cell landscape was thoroughly characterized in patients with IBD before and after treatment with vedolizumab, integrating multiparametric flow cytometry, mass cytometry, and serum proteomics (Olink) data into a predictive model. A predictive signature of Ki67⁺ memory CD4⁺ T cells (area under the curve, 0.97) was increased in nonresponders before treatment, exhibited an activated T-helper 1/T-helper 17 cell phenotype, and was not sufficiently targeted by vedolizumab.

LIMITATIONS

The findings were limited by the modest sample size and need multicenter validation. In addition, the findings were limited to circulating immune cells and not tissues and lack definitive proof of mechanism.

CLINICAL RESEARCH RELEVANCE

Ki67 expression on circulating CD4⁺ memory T cells is a novel pretherapeutic nonresponse feature. This paves the way for a peripheral blood assay for precision therapy in patients with IBD.

BASIC RESEARCH RELEVANCE

This study provides new insights into immune cell characteristics after $\alpha 4\beta 7$ integrin blockade and associated with treatment failure. The findings are particularly relevant in the context of gut homing and recirculation of activated T cells.

treatment. Using machine learning, we identified common features associated with vedolizumab treatment and effectively classified therapy response. Notably, a specific T-cell signature was linked to vedolizumab failure, independent of key clinical variables, such as treatment history or para-clinical parameters. Our findings provide novel insights into the immunologic mechanisms underlying therapy response and failure in patients with IBD treated with vedolizumab.

* Authors share co-first authorship.

Abbreviations used in this paper: AUC, area under the curve; BCR, B-cell receptor; CD, Crohn's disease; CITEseq, cellular indexing of transcriptomes and epitopes by sequencing; CyTOF, cytometry by time of flight; FACS, fluorescence-activated cell sorting; IBD, inflammatory bowel disease; IL, interleukin; ITGB7, integrin subunit $\beta 7$; MAdCAM-1, mucosal vascular addressin cell adhesion molecule 1; PBMC, peripheral blood mononuclear cell; scRNAseq, single-cell RNA sequencing; TCR, T-cell receptor; Th, T-helper; UC, ulcerative colitis; VCAM-1, vascular cell adhesion molecule-1.

 Most current article

© 2025 The Author(s). Published by Elsevier Inc. on behalf of the AGA Institute. This is an open access article under the CC BY-NC-ND license (<http://creativecommons.org/licenses/by-nc-nd/4.0/>).

0016-5085

<https://doi.org/10.1053/j.gastro.2024.09.021>

Materials and Methods

Study Design and Approval

A total of 47 patients (cohort 1; [Supplementary Table 1](#)) and 26 patients (cohort 2; [Supplementary Table 7](#)) receiving vedolizumab at the outpatient and inpatient clinic of the Department of Gastroenterology, Infectiology, and Rheumatology at Charité University Medicine Berlin were enrolled in either a prospective study (VEPREDEX#EA4/162/17) or a prospective biobank (IBDome-study; EA4/162/17), which were approved by the Charité University Medicine Berlin ethics committee. Donors in the first cohort were recruited between July 2018 and November 2021, and patients in the second cohort were included from December 2021 to July 2024. Eligible patients were aged 18–80 years with an established diagnosis of UC or CD. These patients were switched to vedolizumab due to persistently active disease, despite attempts at corticosteroid tapering, or due to a lack of response or intolerance to immunosuppressive medications (such as azathioprine) or tumor necrosis factor antagonists, even after appropriate induction and more than 4 weeks of treatment. Only 6 patients from both cohorts had received ustekinumab before vedolizumab, and none had been treated with JAK inhibitors before starting vedolizumab ([Supplementary Table 16](#) and [Technical Supplementary Figure 10](#)). We also included 41 age- and sex-matched healthy donors (healthy controls) for comparison. All donors provided informed written consent for their participation in the study. In addition to biosampling, we collected relevant (para-) clinical data, including Harvey-Bradshaw Index/partial Mayo Score, C-reactive protein levels, and leukocyte and thrombocyte counts. Responders were classified as patients who achieved a minimum reduction of 3 points in the Harvey-Bradshaw Index and at least 2 points in the partial Mayo score after 30 weeks of vedolizumab treatment.

Peripheral Blood Mononuclear Cell Thawing and Stimulation

PBMCs were thawed in a 37°C water bath, transferred to thawing medium, centrifuged, and resuspended for counting. Cells were used for flow cytometry, surface and transcription factor staining, and stimulated with phorbol myristate acetate/ionomycin for 4 hours. For details, see [Supplementary Experimental Procedures](#).

Flow Cytometry

PBMCs were stained according to standard protocols. For details, see [Supplementary Experimental Procedures](#).

Inhibition of Vascular Cell Adhesion Molecule–1 Binding in Memory CD4⁺ T Lymphocytes

The assay was done as described previously by Soler et al.¹² For details, see [Supplementary Experimental Procedures](#).

Mass Cytometry and Data Processing

Whole blood samples were fixed with PROT1 proteomic stabilizer and stored at –80°C. Upon thawing, samples were stained and acquired in batches of 15, including all time points from the same patient and matched healthy controls. For details, see [Supplementary Experimental Procedures](#).

Single-Cell Sequencing of Peripheral Blood Mononuclear Cells and Data Analysis

Following manufacturer's instructions, single-cell RNA sequencing (scRNAseq) libraries were generated using the Chromium Next GEM Single Cell 5' Reagent Kits, version 2, from 10x Genomics (Pleasanton, CA; CG000330 Rev D). Sequencing libraries for gene expression and T-cell receptor (TCR)/B-cell receptor (BCR) were processed together using Cell Ranger multi (version 5.0.0) and the GRCh38 genome annotation and analyzed using Seurat, version 4.0.11.³¹

Proteomics Serum Assay

Proteomics analysis of patient serum samples was performed using the Olink Target 96 Inflammation panel platform (<https://www.olink.com/products/inflammation/>).

Machine Learning

We applied machine learning techniques to identify markers across 4 data modalities for predicting vedolizumab efficacy in patients with IBD, using logistic regression and cross-validation. The top 10% most influential features were selected, with iterative model validation used to test predictive capacity. Performance was evaluated using area under the curve (AUC) and feature regularization methods (Lasso, ElasticNet) were applied for robustness. For details, see [Supplementary Experimental Procedures](#).

Code Availability

All original code necessary to replicate our analyses, including scRNAseq analyses and machine learning code, are deposited in a GitHub repository (https://github.com/VeroHo/vedo_paper).

Data Availability

All source data relevant to understanding and reproducing the results presented in this article are provided in the [Supplementary Material](#). Sequencing data (scRNAseq, CITEseq, and TCR sequencing) can be accessed at Gene Expression Omnibus (<https://www.ncbi.nlm.nih.gov/geo>) under accession number GSE261334.

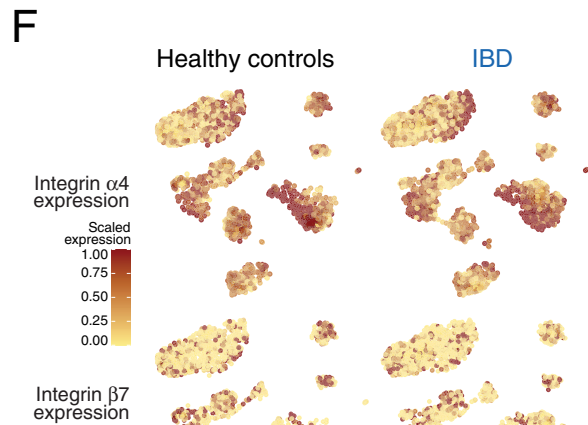
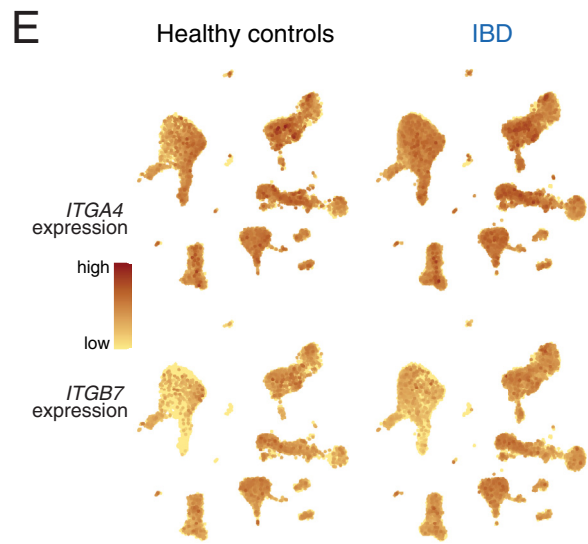
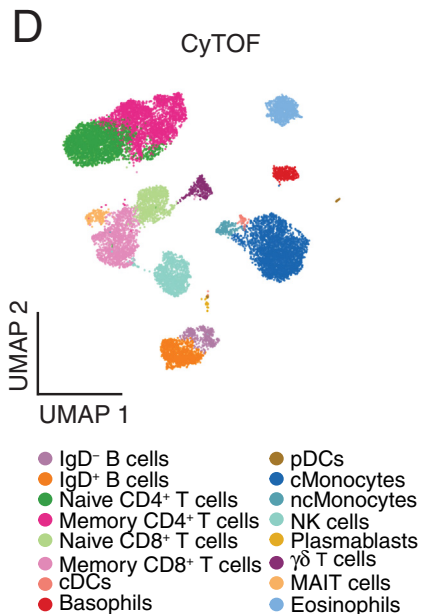
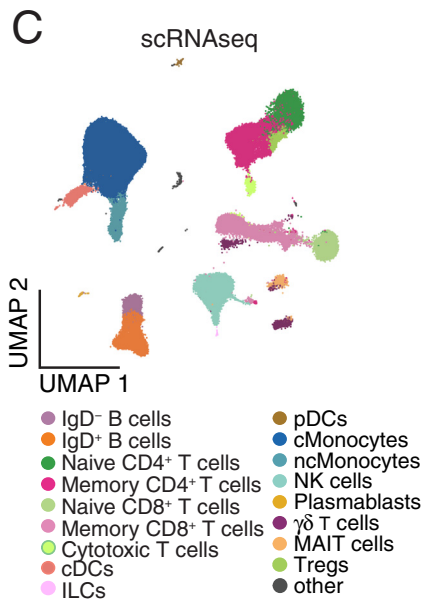
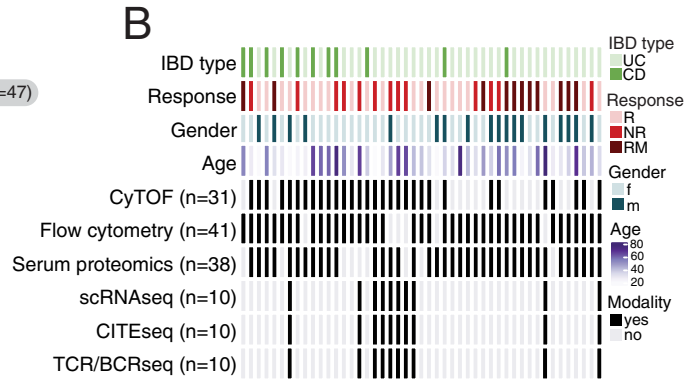
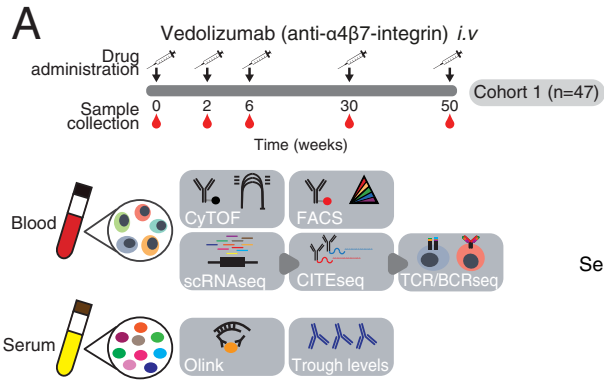
Statistical Analysis

Statistical analyses and visualizations were created in R, using ggpubr (version 0.6.0), ggplot2 (version 3.4.3), limma (version 3.50.3), corrplot (version 0.92), and ComplexHeatmap (version 2.10.0) packages or with Prism software (GraphPad Software). *P* values were calculated using the Wilcoxon test. Paired analyses are indicated by connecting lines.

Results

Multimodal Profiling of Patients With Inflammatory Bowel Disease Receiving Anti-Integrin $\alpha 4\beta 7$ Therapy

We aimed to investigate the effect of vedolizumab treatment on circulating immune cells at baseline and during treatment. Therefore, we prospectively sampled blood from a cohort of patients with IBD receiving vedolizumab at



baseline and during treatment (IBD, $n = 47$; Figure 1A, Supplementary Table 1) together with age- and sex-matched healthy controls ($n = 41$; Supplementary Figure 1A, Supplementary Table 1). We recorded disease activity scores, prior treatments, and paraclinical parameters (Supplementary Figure 1B–E, Supplementary Table 16). Responders were classified as patients who achieved a minimum reduction of 3 points in the Harvey-Bradshaw Index (for CD) and at least 2 points in the partial Mayo score (for UC) after 30 weeks of vedolizumab treatment and continued vedolizumab treatment. Stool calprotectin levels at 18 weeks effectively distinguished responders from nonresponders (Supplementary Figure 1D).

Mass cytometry was used to profile whole blood, identifying and characterizing immune cell subsets of major innate and adaptive populations with 36 protein targets (Supplementary Tables 10 and 11). Serum samples underwent proteomic analysis using the Olink proximity extension assay (Target 96 Inflammation panel, Supplementary Table 14) to detect changes in inflammatory markers before and 6 weeks after treatment induction (Figure 1A and B). In a selected sub-cohort, PBMCs were analyzed using single-cell sequencing and immune repertoire profiling to evaluate gene and protein expression (CITEseq) and to monitor changes in TCR and BCR repertoires upon treatment (Supplementary Tables 12 and 13). In addition, multiparametric flow cytometry (fluorescence-activated cell sorting [FACS]) was used to examine the expression of chemokine receptors, surface molecules, integrins, cytokines, and transcription factors in circulating T cells (Figure 1B, Supplementary Tables 8 and 9).

Integrin $\alpha 4\beta 7$ Expression and Distribution on Circulating Immune Cells at Steady-State and After Treatment

We first obtained a comprehensive overview of the circulating immune cell landscape in healthy controls and patients with IBD. CITEseq analysis and mass cytometry identified approximately 16–18 different cell clusters (Figure 1C and D, Supplementary Figures 2A and B and 3A and B). Both datasets revealed that patients with IBD have an altered immune cell composition compared with healthy controls (Supplementary Figures 2C and 3C). Next, we performed a comprehensive single-cell analysis of $\alpha 4\beta 7$ integrin expression in both healthy and diseased conditions

(Figures 1E and F and 2A and B). The scRNAseq analysis revealed *ITGA4* (integrin $\alpha 4$) and *ITGB7* (integrin $\beta 7$) expression across all lineages (Figure 1E and 2A). *ITGA4* showed high expression across all major cell types (Figures 1E and 2A), although there was differential *ITGB7* expression on specific immune cells (Figures 1E and 2A). *ITGA4* and *ITGB7* expression were similar between healthy controls and patients with IBD (Figure 2A and Supplementary Figure 4A).

We next explored the protein expression of integrin $\alpha 4$ and $\beta 7$ on circulating immune cells to identify cell lineages potentially targeted by vedolizumab. In our CITEseq dataset, integrin $\beta 7$ protein expression (ADT, antibody-derived tag) showed a similar distribution to *ITGB7* RNA expression (Figure 2B). Gating on $\alpha 4\beta 7$ co-expressing cells in the mass cytometry dataset and performing cell clustering within this subset (Figure 2C and Supplementary Figure 4B), we found that $\alpha 4$ and $\beta 7$ integrins were co-expressed not only in T cells and monocytes, but also in other cell lineages, with CD4/CD8⁺ T cells and eosinophils being the most abundant (Figure 2C). The frequency of $\alpha 4\beta 7$ ⁺ cells was significantly reduced in patients with IBD before treatment induction across several cell types (Supplementary Figure 4C and D). Surprisingly, protein expression of integrin $\beta 7$, but not integrin $\alpha 4$, was up-regulated after vedolizumab treatment in all cell subsets (Figure 2B and D), with significant changes in memory CD4⁺ and CD8⁺ T cells, eosinophils, classical monocytes, memory B cells, basophils, conventional dendritic cells, and natural killer cells (Figure 2E).

Taken together, our data demonstrated that integrin $\alpha 4\beta 7$ is expressed on various circulating cell lineages and that vedolizumab modulates expression of integrin $\beta 7$.

Vedolizumab Enhances Clonal Diversity in Circulating Memory T Cells

Targeting memory T cells expressing integrin $\alpha 4\beta 7$ is a key mechanism by which vedolizumab modulates intestinal inflammation.¹³ Animal studies suggest that anti-integrin $\alpha 4\beta 7$ treatment releases gut-resident immune cells into circulation.^{5,11,14} To test this, we assessed the diversity of circulating T and B cells before and after treatment using single-cell TCR and BCR repertoire analysis (TCR/BCR sequencing) combined with CITEseq (Figure 3A and B, Supplementary Figure 5A and F). We found a significant increase in clonal diversity, specifically in memory CD4⁺ T cells, but not CD8⁺ T cells and B-cell subsets after treatment

Figure 1. Multimodal characterization of patients with IBD receiving anti-integrin $\alpha 4\beta 7$. (A) Study design. (B) The study cohort and analyses applied to each patient sample (UC, CD; response: responder [R], nonresponder [NR], remission maintenance [RM]; gender, age). (C) Uniform Manifold Approximation and Projection (UMAP) plots of CITEseq profiled peripheral blood cells with color-coded representation of cell types and patients ($n = 191,578$ cells derived from a total of 25 samples: healthy controls [HC], $n = 5$; IBD, $n = 10$ matched before and after treatment). Sorted CD45⁺ cells from the peripheral blood of 5 healthy controls and 10 patients with UC before and 6 weeks after vedolizumab (VDZ) treatment initiation were subjected to CITEseq analysis. cDC, conventional dendritic cell; ILC, innate lymphoid cell; MAIT, mucosal-associated invariant T cell; NK, natural killer; pDC, plasmacytoid dendritic cell; Treg, regulatory T cell. (D) UMAP plots of peripheral blood cells extracted from the CyTOF dataset, with color representation based on cell type and patient. Results derived from FlowSOM/ConsensusPlus clustering analysis performed on 13,311,287 cells from 154 samples. This dataset includes both HCs and patients with IBD both before and during treatment. (E) Expression of *ITGA4* and *ITGB7* in the different cell subsets derived from scRNAseq data. (F) Scaled expression of integrin $\alpha 4$ and $\beta 7$ in the CyTOF dataset from HCs and patients with IBD before therapy (IBD).

(Figure 3C, Supplementary Figure 5B and G). After treatment, there was an increase in TCR diversity, specifically in central memory CD4⁺ T cells, but not in effector memory CD4⁺ T cells or in the corresponding CD8⁺ T-cell populations (Figure 3D and Supplementary Figure 5B). Using

the scRNAseq dataset, we investigated whether anti-integrin $\alpha 4\beta 7$ treatment specifically affects TCR diversity in gut-homing T-cell subsets. We found a significant increase in TCR diversity in CD4⁺ T cells expressing *ITGA4* and *ITGB7*, but not in those expressing *ITGB1*, *GPR15*, or *ITGAE*

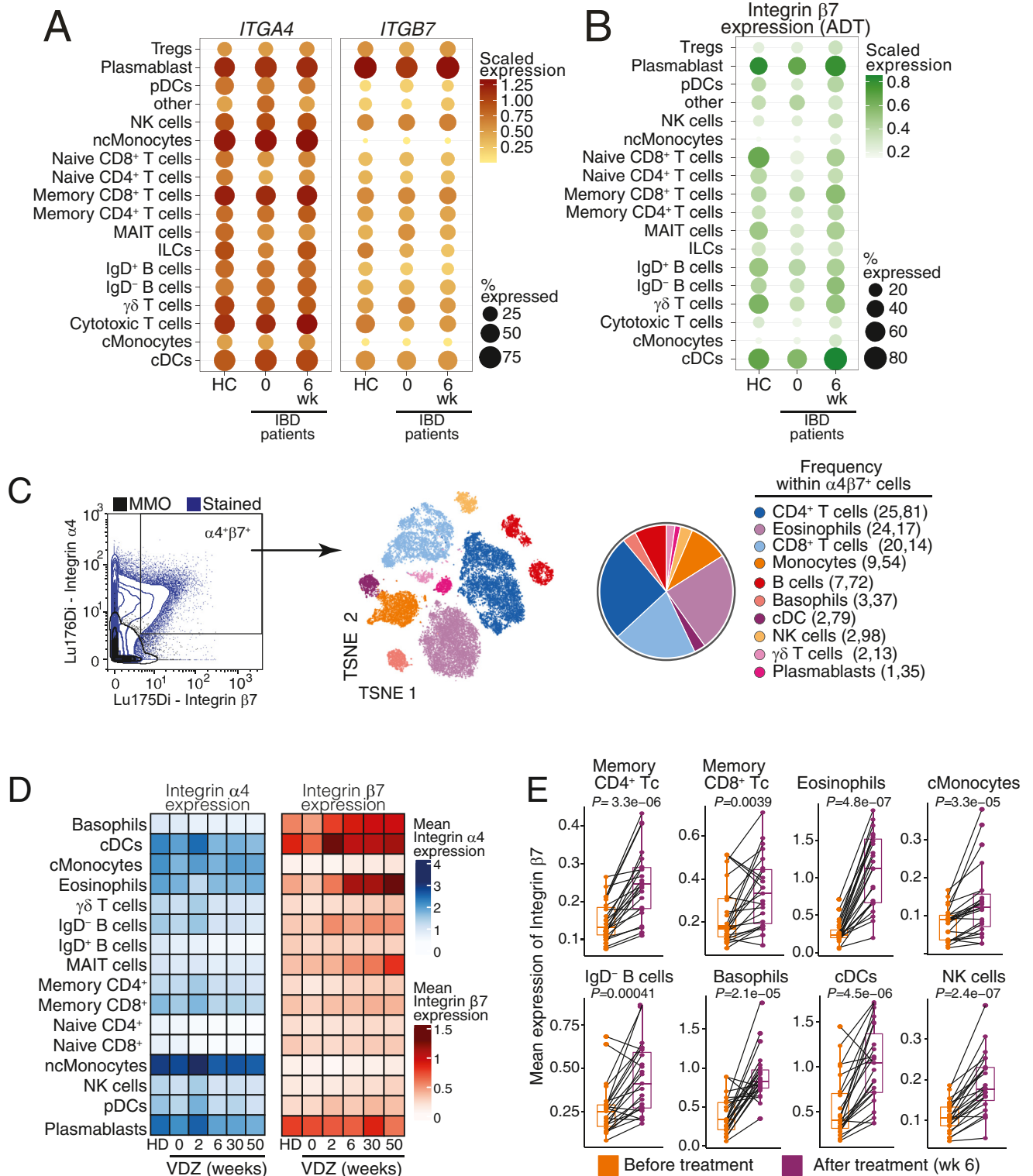


(Figure 3E and F and Supplementary Figure 5A). However, treatment did not increase TCR diversity among gut-homing CD8⁺ T cells (Supplementary Figure 5C and D). There were no specific alterations in TCR and BCR diversity based on therapy response (Supplementary Figure 6A and B). Consistent with the increase in TCR diversity of CD4⁺ T cells, memory CD4⁺ T cells (but not CD8⁺ or B cells) also significantly increased after treatment (Figure 3G–I, Supplementary Figure 5E, H, and I).

These findings provide evidence that vedolizumab significantly increases clonal diversity within circulating memory T cells, with a particular impact on central memory and $\alpha 4\beta 7^+$ memory CD4⁺ T cells.

Vedolizumab Modulates the Abundance of Circulating $\alpha 4\beta 7$ -Integrin⁺ Immune Cells and Proinflammatory Serum Proteins

We next integrated our multimodal datasets into a reductionist machine learning model, focusing on cytometry by time of flight (CyTOF), FACS, and Olink data to gain a comprehensive understanding of vedolizumab's immunologic effects in the circulation of patients with IBD. Due to observed changes in their TCR diversity, we focused our flow cytometry analysis on memory CD4⁺ T cells (Figure 4A, Supplementary Table 2, Supplementary Figures 7 and 8).

Using a logistic regression classifier, we found that vedolizumab treatment significantly increased the abundance of integrin $\alpha 4\beta 7$ on circulating immune cells (CyTOF- $\alpha 4\beta 7$; AUC, 0.97; Figure 4B). The abundance of $\alpha 4\beta 7^+$ cells in the bloodstream increased over time with vedolizumab treatment (Figure 4C), especially in populations with the highest integrin $\alpha 4\beta 7$ expression (Figures 4D and E). The second major effect of vedolizumab was observed in inflammatory serum protein levels at week 6 after treatment initiation (Olink; AUC, 0.94; Figure 4B). Unexpectedly, several serum proteins, including eotaxin (CCL11), delta/notch-like epidermal growth factor-related receptor, chemokine (C-X3-C motif) ligand (CX3CL) 1, tumor necrosis factor- β (or LT- β), and chemokine (C-C motif) ligand (CCL) 28, showed significant increases after vedolizumab treatment (Figures 4F and G, Supplementary Figure 9A–C). To explore the mechanism underlying this phenomenon, we analyzed gene expression corresponding to the inflammatory serum proteins in the intestinal mucosa of patients with IBD treated with vedolizumab in RNAseq data

from the GEMINI trial (GSE73661).¹⁰ In the intestinal mucosa, the genes corresponding to the Olink proteins were not up-regulated after vedolizumab treatment, suggesting that the increased protein serum levels cannot be attributed to enhanced expression of these genes in inflamed tissue (Supplementary Figure 10A–C). However, we found a positive correlation between the top serum markers and the abundance of the most altered $\alpha 4\beta 7$ -expressing populations identified by mass cytometry, suggesting that immune cell entrapment after anti-integrin treatment may explain the increased serum inflammatory markers (Figure 4H).

In conclusion, vedolizumab strongly alters the abundance of circulating immune cells, particularly those expressing high levels of $\alpha 4\beta 7$ integrin, and this is associated with increased inflammatory serum markers.

Integration of Multimodal Data Identifies Determinants of Nonresponse to Anti-Integrin Treatment

We applied both linear and nonlinear classification approaches to the multiparametric data (Figure 5A, Supplementary Figure 11A and B, and Supplementary Table 15) to identify features associated with vedolizumab nonresponse. After evaluating performance and model simplicity, we selected logistic regression as the final method for classifying treatment outcomes (Supplementary Figure 11A–C, Supplementary Table 3).

Surprisingly, when we analyzed all measured parameters (features) from individual modalities (eg, FACS, Olink, CyTOF, CyTOF- $\alpha 4\beta 7$), we were unable to successfully classify therapy outcomes (Figure 5B and Supplementary Figure 11D, upper left, Supplementary Table 3). In addition, combining all modalities did not improve classification performance (Figure 5B and Supplementary Figure 11D, lower left). However, selecting the top 10% of features from each modality significantly improved classification accuracy (Figure 5B and Supplementary Figure 11E). We achieved an AUC of 0.89 for Olink and 0.91 for FACS individually (Figure 5B and Supplementary Figure 11D, upper right). Combining the top 10% of features from both modalities further improved performance, reaching an AUC of 0.98 (Figure 5B and Supplementary Figure 11D, lower right).

Testing the 4 best-performing models using an iterative approach resulted in the validation of the models containing

Figure 2. Integrin $\alpha 4\beta 7$ expression and distribution in circulating immune cells at steady-state and modulation upon anti-integrin $\alpha 4\beta 7$ treatment. (A) Dot plot of *ITGA4* and *ITGB7* expression in scRNAseq data from different cell types and different conditions before treatment (0) and 6 weeks (6 wk) after treatment. *Color* indicates expression level, *dot size* indicates the percentage of positive cells. cDC, conventional dendritic cell; ILC, innate lymphoid cell; MAIT, mucosal-associated invariant T cell; NK, natural killer; pDC, plasmacytoid dendritic cell; Treg, regulatory T cell. (B) As in (A), derived from integrin $\beta 7$ protein expression (antibody-derived tag [ADT]) by CITEseq. (C) Representative dot plot of integrin $\alpha 4$ (CD49d) and $\beta 7$ staining in mass cytometry on CD45⁺ cells showing stained cells (*blue*) and metals-minus-one (MMO) control. T-distributed stochastic neighbor embedding (TSNE) with results of FlowSOM clustering of $\alpha 4\beta 7^+$ cells from the mass cytometry dataset and a pie chart representing the percentage of cluster frequency within the total $\alpha 4\beta 7^+$ cells derived from healthy controls (HCs) and patients with IBD. (D) Mean integrin $\alpha 4$ and $\beta 7$ expression within mass cytometry clusters, as determined by the FlowSOM algorithm in healthy donors (HDs) and patients with IBD before treatment and at the indicated time points after treatment initiation (HDs, n = 27; before treatment, n = 31; week 2, n = 9; week 6, n = 25; week 30, n = 15; week 50, n = 9). (E) Comparison of mean integrin $\beta 7$ expression in indicated mass cytometry cluster before and 6 weeks after treatment. *P* values were calculated using the paired Wilcoxon test.

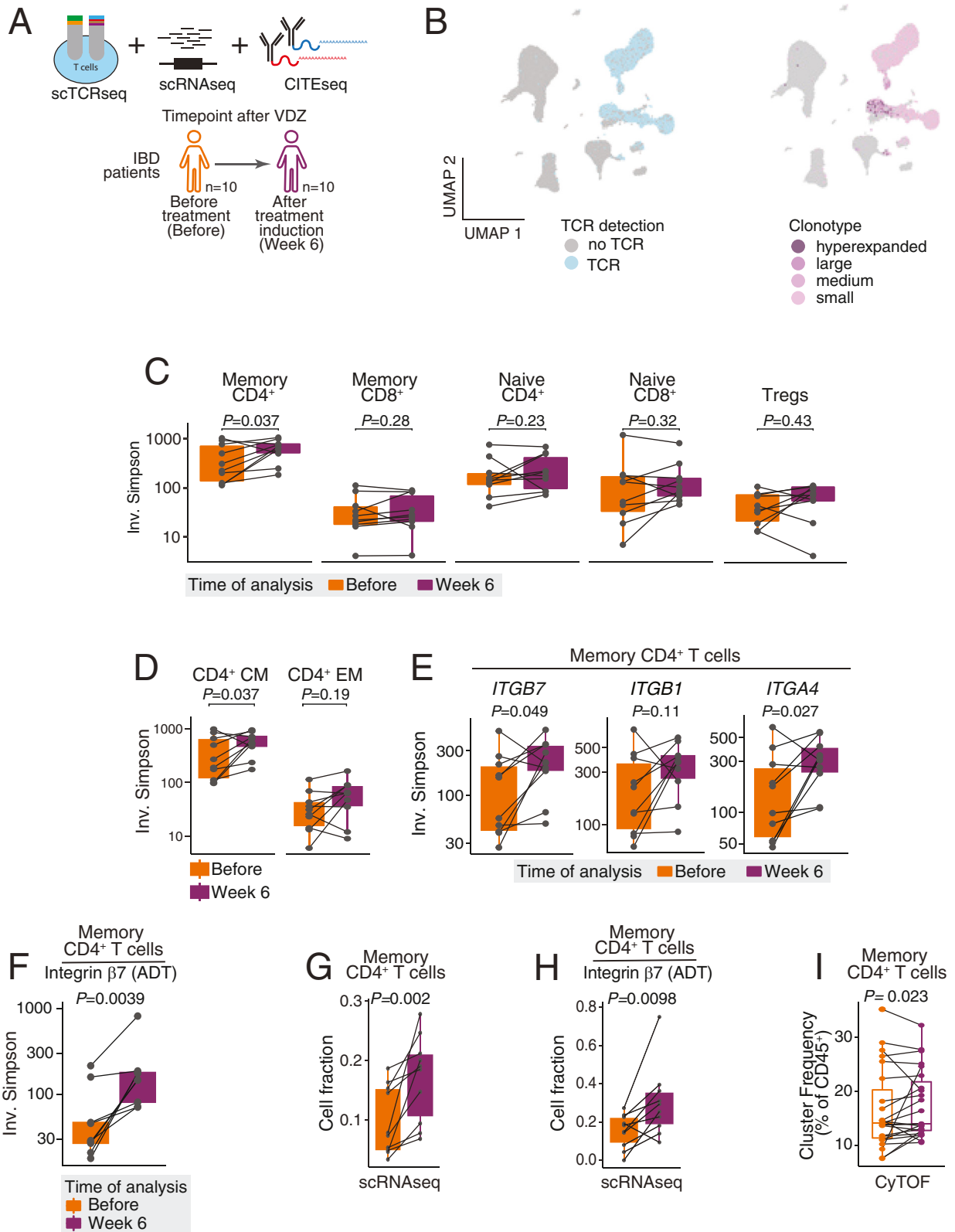
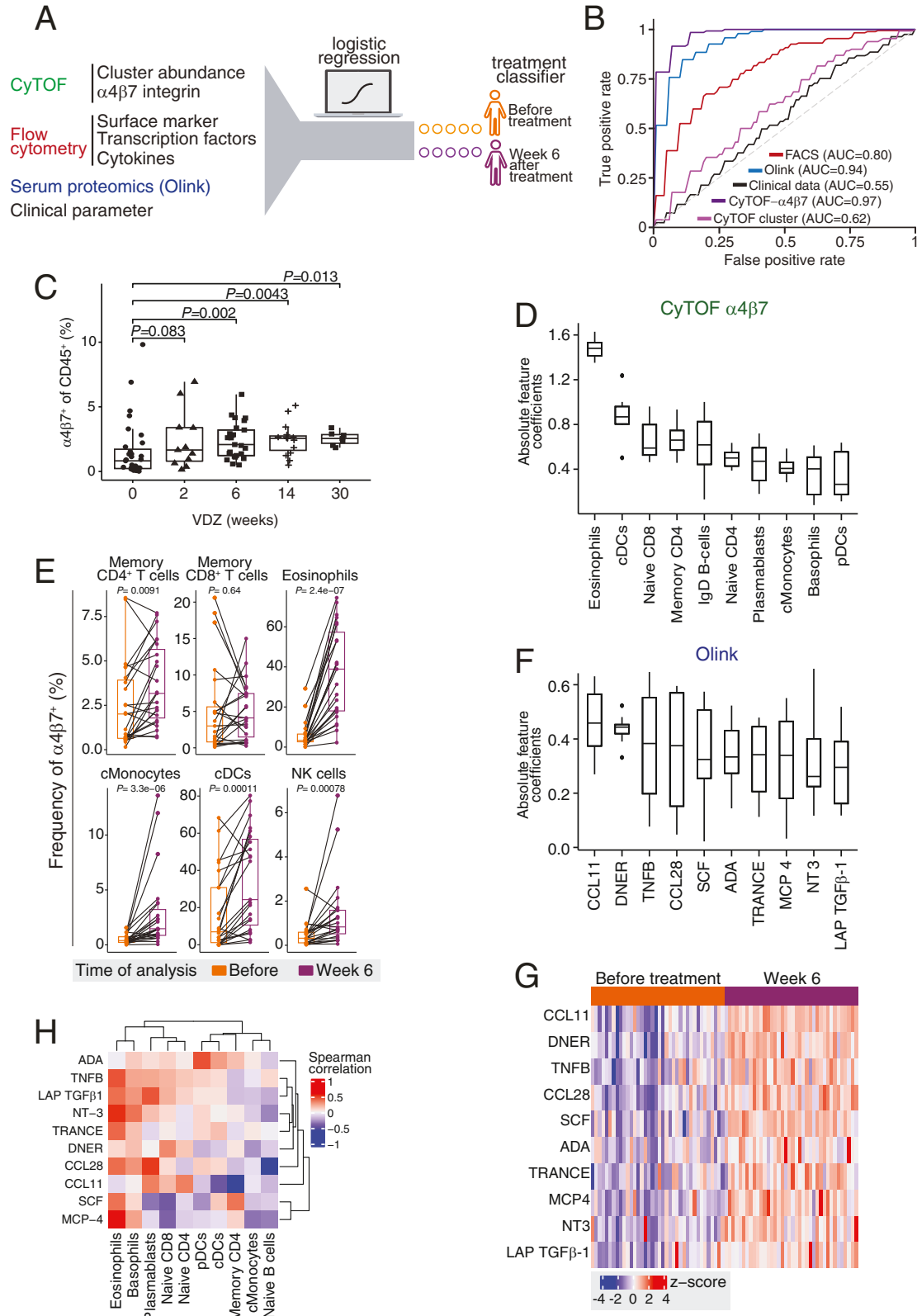


Figure 3. Vedolizumab enhances clonal diversity among circulating CD4⁺ memory T cells. (A) Schematic of the experimental approach. (B) Uniform Manifold Approximation and Projection (UMAP) plot indicating cells with detected TCR sequence (left) and frequency of the associated clonotype (right; small: $< 10^{-3}$, medium: $< 10^{-2}$, large: $< 10^{-1}$, hyperexpanded: $> 10^{-1}$). (C) Clonal diversity quantified by the inverse Simpson index in various T-cell subsets before treatment and 6 weeks after treatment. Treg, regulatory T cell. (D) Clonal diversity in central and effector memory CD4⁺ T-cell subpopulations. (E) Clonal diversity in memory CD4⁺ T-cell subpopulations defined by expression of the indicated marker genes. (F) Clonal diversity in memory CD4⁺ T cells with positive integrin $\beta 7$ expression (antibody-derived tag [ADT]) determined by CITEseq. (G) Abundance of memory CD4⁺ T cells among all sequenced cells per sample. (H) Abundance of memory CD4⁺ T cells with positive integrin $\beta 7$ expression determined by CITEseq. (I) Cluster frequency in the mass cytometry dataset. (C–I) Wilcoxon test.

(1) Olink/FACS, (2) Olink/FACS/CyTOF, and (3) FACS/CyTOF/clinical parameters, although FACS/CyTOF- $\alpha 4\beta 7$ did not reach the required test accuracy >0.5 (Supplementary Figure 12A). For each of the 3 validated models, we

selected the top 5 features with highest absolute feature coefficients (Figure 5C and Supplementary Figure 12B), which also emerged from a similar analysis using automatic feature selection methods (Supplementary Figure 12C,



Supplementary Table 4), and used the resulting refined models for classification of treatment response (Figure 5D). Parameters within memory CD4⁺ T cells, including chemokine receptors, cytokines, serum inflammatory markers, abundance of natural killer cells in the circulation measured by mass cytometry, and especially the proliferation marker Ki67, had a high influence on predictive capacity. An AUC of 0.99 was achieved by selecting a panel containing the top 3 features in the FACS/Olink/CyTOF model (Figure 5D), while still maintaining test set accuracies of 0.75. Here, classification performance remained compelling even when tested on a reduced patient set (Supplementary Figure 12D, Supplementary Table 5). Remarkably, evaluating the predictive capacity of Ki67⁺ memory CD4⁺ T cells alone in the FACS/Olink/CyTOF model yielded an AUC of 0.93, thus scoring higher than the majority of top-3 and top-5 feature combinations.

To test the reproducibility of these findings, we next recruited a validation cohort of patients with IBD undergoing vedolizumab treatment (n = 26) and analyzed PBMCs using an optimized and simplified flow cytometry panel. In that cohort, the combination of our top 3 FACS markers (Ki67, CXCR3, and IL4) achieved an AUC of 0.99 (Figure 5E).

Thus, our 3-feature FACS panel on Ki67⁺ memory CD4⁺ T cells allowed reliable prediction of treatment response, and we identified the abundance of proliferating CD4⁺ memory T cells in circulation as a key classifier of vedolizumab treatment outcome.

Transcriptional Characteristics of Circulating Ki67⁺ Effector CD4⁺ T Cells

To further investigate the observed increase in T-cell proliferation in vedolizumab nonresponders, we analyzed different T-cell populations for Ki67 expression. We observed significant enrichment of Ki67⁺ cells within total CD3⁺ T cells in the blood of nonresponders (Supplementary Figure 13A). This increased Ki67⁺ fraction was specific to memory CD4⁺ T cells (but not regulatory or memory CD8⁺ T cells) in nonresponders compared with responders in both patients with UC and patients with CD (Supplementary Figure 13A–C). This finding was also confirmed in the validation cohort (Supplementary Figure 13D). Interestingly, Ki67⁺ levels in memory CD4⁺ T cells were significantly elevated in patients with IBD before therapy initiation and

remained unaffected by vedolizumab (Supplementary Figure 13E and F).

To further characterize Ki67⁺ memory CD4⁺ T cells, we conducted additional single-cell sequencing analysis on FACS sort-purified memory CD4⁺ T cells from the same donors used initially in our study, which was integrated with the pre-existing PBMC scCITEseq data (Figure 6A and Figure 1B). Hierarchical clustering resulted in 12 distinct clusters within the sequenced memory CD4⁺ T cells (Figure 6B, Supplementary Figure 14A–C), with predominant enrichment of Ki67⁺ memory CD4⁺ T cells in cluster 1 (Figure 6C and D), which, consistent with our FACS data, was significantly increased in nonresponders before treatment (Figure 6E).

We compared the genes expressed in cluster 1 with all other clusters (Figure 6F, Supplementary Table 6), focusing on classical activation and homing markers, cytokine receptors, cytokines, and classical T cell–related transcription factors (Figure 6G). Our analysis revealed signs of activation and proliferation in cluster 1 (up-regulated *HLADRA*, *CD40LG*, and *MKI67*, down-regulated *IL7R* and *SELL*) (Figure 6G, activation markers, and cytokine receptors). Furthermore, cells in cluster 1 showed high *ITGA4*, *ITGB1*, and *ITGB7* levels, and *CXCR3* and *CCR6* (Figure 6G, homing receptors) expressed *IL12BR2*, *IL18R1*, and showed down-regulation of *IFNGR2* (Figure 6G, cytokine receptors). Several transcription factors, including *TBX21*, *RORC*, *MAF*, and *TOX*, were up-regulated (Figure 6G, transcription factors). By integrating protein data, we confirmed that cluster 1 expressed increased protein levels of HLA-DR, while displaying low expression of CD25, CD45RA, and CD127 (Figure 6H). Our findings indicate that Ki67⁺ memory CD4⁺ T cells constitute an activated subpopulation distinguished by T-helper (Th) 1 and Th17 attributes, elevated integrin expression, heightened gut-homing potential, and increased activation markers.

Proliferating Effector Memory CD4 T Cells Exhibit Expression of Alternative Homing Receptors and T-helper 1/T-helper 17 Cell Characteristics

We used multiparametric flow cytometry to explore the functional characteristics of the predictive Ki67⁺ effector memory CD4⁺ T-cell signature in IBD, including markers identified by single-cell sequencing. There was a positive

Figure 4. Vedolizumab (VDZ) modulates integrin $\alpha 4\beta 7$ expression on circulating immune cells, cell type abundance, and proinflammatory serum proteins. (A) Machine learning approach used to identify the effects of VDZ treatment on circulating immune cells. (B) Capacity of clinical parameters, Olink, mass cytometry, and flow cytometry data to display VDZ treatment signatures shown as receiver operating characteristic curves (ROC) with corresponding AUC values. (C) Percentage of $\alpha 4\beta 7^+$ cells from total CD45⁺ cells in the mass cytometry dataset at different time points throughout treatment (patients with IBD before treatment, n = 31; week 2, n = 9; week 6, n = 25; week 30, n = 15; week 50, n = 9). Mann-Whitney test. (D) Overview of the top 10 VDZ efficacy features from the CyTOF- $\alpha 4\beta 7$ dataset with the largest feature coefficients. These populations have the highest feature coefficients, and the absolute values of these coefficients are shown. The complete list can be found in Supplementary Table 3. cDC, conventional dendritic cell; pDC, plasmacytoid dendritic cell. (E) Percentage of $\alpha 4\beta 7^+$ cells from total CD45⁺ per indicated cluster in the mass cytometry dataset from week 0 vs week 6 (patients with IBD before treatment, n = 31; after treatment, n = 25). Paired Wilcoxon test. NK, natural killer. (F) Overview of the 10 VDZ efficacy features from Olink data with the largest feature coefficients. DNER, delta/notch-like epidermal growth factor-related receptor. (G) Olink quantification of the indicated analytes before treatment (n = 39) and 6 weeks after VDZ treatment (n = 39). (H) Spearman correlation between the serum proteomics' most significantly altered cytokines and the abundance of cell populations measured by CyTOF after treatment.

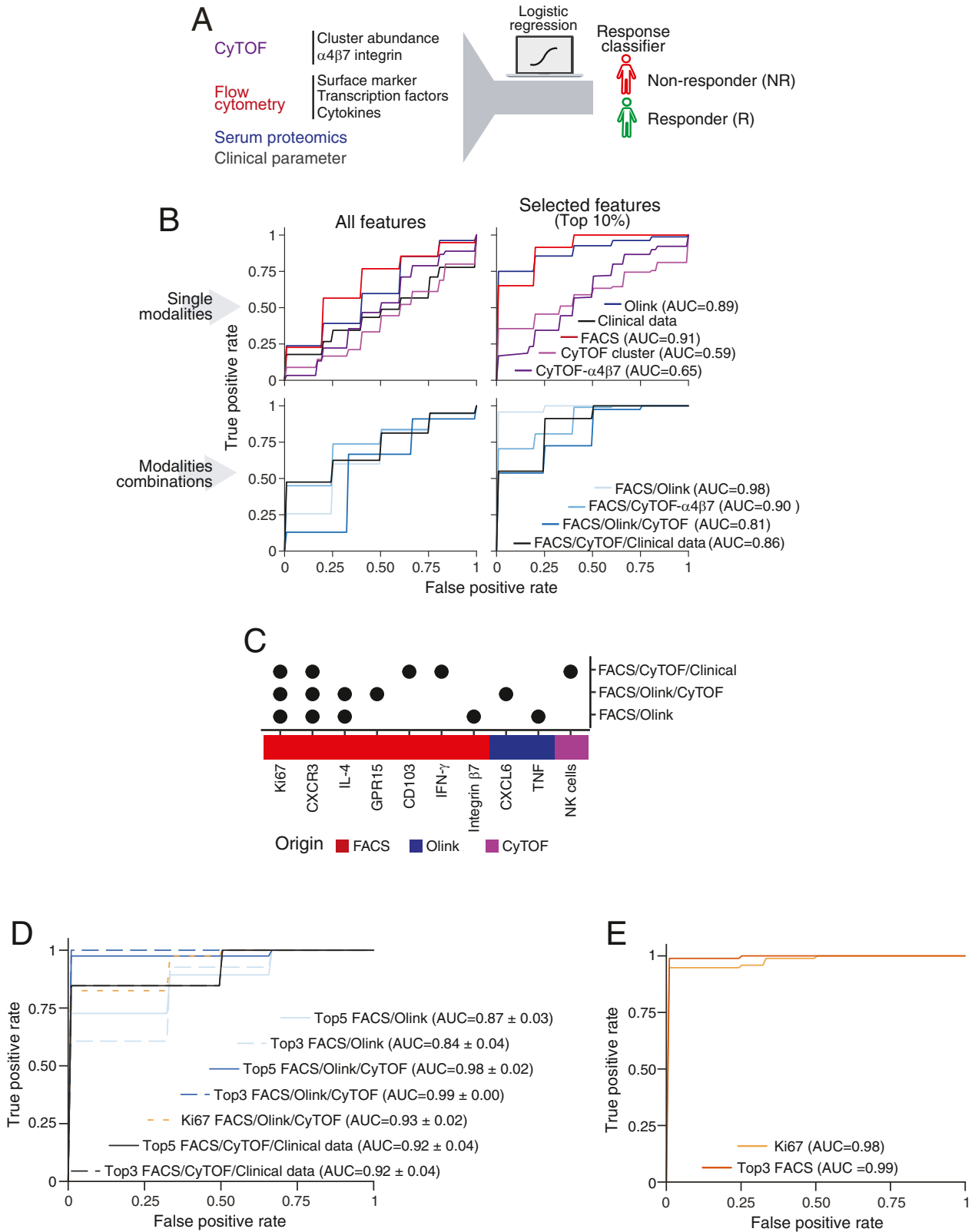
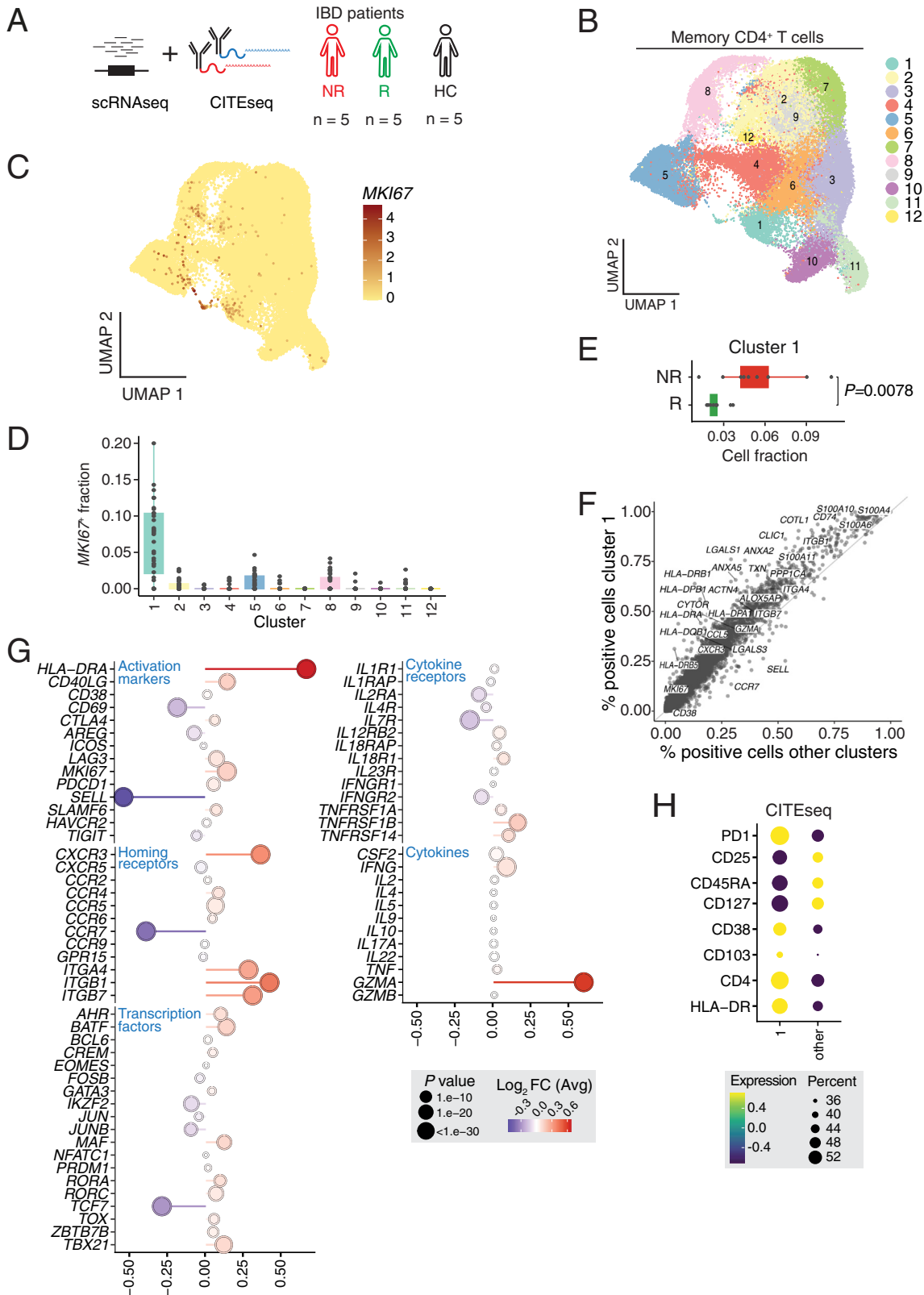


Figure 5. Machine learning–based classification identifies vedolizumab-induced immune changes and classifies therapy response. (A) Machine-learning approach used to identify the effects of vedolizumab treatment on circulating immune cells and to classify treatment response. (B) Predictive capacity of individual data sets (*top*) and data combinations showing the highest AUC values (*bottom*) to classify vedolizumab response. Classifications are performed using all features (*left*) or the top 10% most predictive features from the ranked logistic regression coefficients (*right*). (C) Occurrence of the 5 most predictive features across the validated best-performing models, see also [Supplementary Figure 12B](#). IFN, interferon; NK, natural killer; TNF, tumor necrosis factor. (D) Predictive capacity of selected marker combinations from the validated top-performing models (cf [Supplementary Figure 12A](#)). (E) Biomarker validation in an independent cohort of patients with IBD treated with vedolizumab (n = 26). As indicated, the predictive capacity is shown using Ki67 or the top 3 most frequent FACS markers (ie, Ki67, CXCR3, and IL-4).

correlation between Ki67 and HLA-DR, CD38, and PD-1 expression (Supplementary Figure 15A). Ki67⁺ memory CD4⁺ T cells showed increased expression of HLA-DR, CD38,

and PD-1 and decreased expression of CD127 and CCR7 compared with Ki67⁻ cells (Figure 7A-C; Supplementary Figure 15A-C). These cells also expressed high levels of



integrin $\alpha 4$ and $\beta 1$, with nearly 80% expressing integrin $\alpha 4\beta 1$ and 20% expressing integrin $\alpha 4\beta 7$ (Figure 7A–C). Indeed, vedolizumab did not inhibit interactions between integrin $\alpha 4\beta 1$ and its ligand vascular cell adhesion molecule (VCAM) (Supplementary Figure 15E–G). In addition, Ki67⁺ memory CD4⁺ T cells expressed high levels of GPR15, CXCR3, and CCR6, which are critical for migration to inflamed sites (Supplementary Figure 15B and C), consistent with the high expression of corresponding chemokine ligands and adhesion molecules in inflamed intestinal tissue (Supplementary Figure 16).

Expression of Th1/Th17 transcription factors T-bet, Eomes, ROR γ t, and the cytokine IL-17A were also increased in Ki67⁺ memory CD4⁺ T cells (Figure 7D and E; Supplementary Figure 15D). In vedolizumab non-responders, there was an increase in T-bet⁺ROR γ t⁺ cells and a reduction in FoxP3 expression within Ki67⁺ memory CD4⁺ T cells (Figure 7F). These findings collectively demonstrate that Ki67⁺ memory T cells are significantly enriched in the blood of patients who fail to respond to anti-integrin therapy, express $\alpha 4\beta 1$ integrin, and exhibit an activated Th1/Th17 phenotype.

Discussion

This study investigated the impact of anti-integrin $\alpha 4\beta 7$ treatment on the circulating immune cell landscape in IBD and identified factors associated with nonresponse. First, $\alpha 4\beta 7$ integrin was expressed across various immune cell types, including both innate and adaptive circulating immune cells, leading to significant alterations in their composition and expression of $\alpha 4\beta 7$ integrin after therapy initiation. Second, the TCR repertoire of CD4⁺ T cells, specifically effector and $\alpha 4\beta 7$ ⁺ memory CD4⁺ T cells, changed after treatment. Third, integrating acquired multimodal parameters into a composite model effectively classified therapy response to vedolizumab. Fourth, the predictive activated cycling effector CD4 T-cell subset expressed molecules associated with pathogenic Th1/Th17 responses, including the transcription factors T-bet and ROR γ t and homing markers, including CXCR3, CCR6, and integrin $\alpha 4\beta 1$. Finally, we confirmed that the abundance of circulating proliferating effector CD4⁺ T cells is a novel classifier of vedolizumab failure in patients with IBD.

Vedolizumab is thought to reduce intestinal inflammation by modulating T cell migration and entry to the gut. Notably, gut-resident CD4⁺ T cells can migrate from gut tissue into the circulation.³² Vedolizumab treatment may disrupt their re-entry into the gut, possibly leading to

retention of circulating gut-resident CD4⁺ T cells in the peripheral blood. This phenomenon could account for the observed enhancement in clonal diversity among circulating CD4⁺ T cells. However, its effects on the abundance and activation of intestinal T cells and the colonic TCR repertoire have been described as minor.³³

Our findings reveal broad $\alpha 4\beta 7$ integrin expression on a variety of immune cell types, but $\alpha 4\beta 7$ integrin levels changed most significantly in circulating myeloid populations after treatment. Transcriptional analysis of whole colonic biopsies acquired before and after vedolizumab treatment previously suggested that vedolizumab primarily affects innate rather than adaptive immunity.³³ Indeed, inflammation-adapted emergency hematopoiesis, increased bone marrow output, and skewing toward enhanced granulocyte-monocyte progenitors have been found to occur and support intestinal inflammation, and these granulocytic populations express integrin $\alpha 4\beta 7$ and migrate to mucosal tissues.^{34,35} Consistent with these data, we observed an increased abundance of circulating eosinophils, monocytes, and dendritic cells after vedolizumab treatment, irrespective of therapy response. These findings suggest that by targeting $\alpha 4\beta 7$ integrin, vedolizumab potentially reduces infiltration of newly generated myeloid cells into gut tissue.

Because the influence of vedolizumab treatment on the systemic inflammatory environment in patients remains unclear, we measured proinflammatory serum proteins before therapy initiation and 6 weeks later. We observed significant alterations in serum proinflammatory markers in patients with IBD compared with healthy controls. Of particular interest, we noted an increase in several serum markers after 6 weeks of vedolizumab, consistent with preclinical observations in rhesus macaques.¹⁵ Interestingly, we found a strong correlation between the top-enriched serum analytes and the abundance of various cellular populations also enriched in peripheral blood after vedolizumab treatment. This suggests that the sequestration of inflammatory cells in the circulation may contribute to proinflammatory cytokine and chemokine release.

Ki67⁺ memory CD4⁺ T cells were enriched in patients with IBD compared with healthy controls, and these cells were significantly increased in nonresponders to vedolizumab. Furthermore, these cells co-expressed activation markers CD38 and HLA-DR, which are increased in the blood and colonic mucosa of patients with IBD.³⁶ Ki67⁺ memory CD4⁺ T cells showed reduced CD127 and CCR7 expression, while HLA-DR and CD38 expression was increased, confirming their activation and effector status. Indeed,

Figure 6. Enrichment of proliferating Ki67⁺ effector CD4⁺ T cells in vedolizumab-refractory patients. (A) Schematic depiction of experimental approach. (B) Uniform Manifold Approximation and Projection (UMAP) plot of CD4⁺ memory cells using combined PBMC and CD4⁺-sorted scRNAseq data from 5 HCs and 10 patients with IBD. (C) Normalized expression of *MKI67* in CD4⁺ memory cells. (D) Fraction of *MKI67*⁺ cells within different clusters. (E) Fraction of *MKI67*⁺ cells in cluster 1 for responders (R) and nonresponders (NR), respectively. Mann-Whitney test. (F) Scatter plot of marker genes for cluster 1 showing percentage of cells with detectable expression in cluster 1 compared with all other clusters. (G) Lollipop graph illustrating fold expression of selected genes in cluster 1 compared with other clusters. The *color scale* represents the mean log₂-fold expression, and the *dot size* represents the *P* value. Genes are categorized according to different functions, including activation markers, cytokine receptors, transcription factors, cytokines, and homing receptors. (H) Dot plot displaying scaled CITEseq expression of selected markers in cluster 1 in comparison with other clusters.

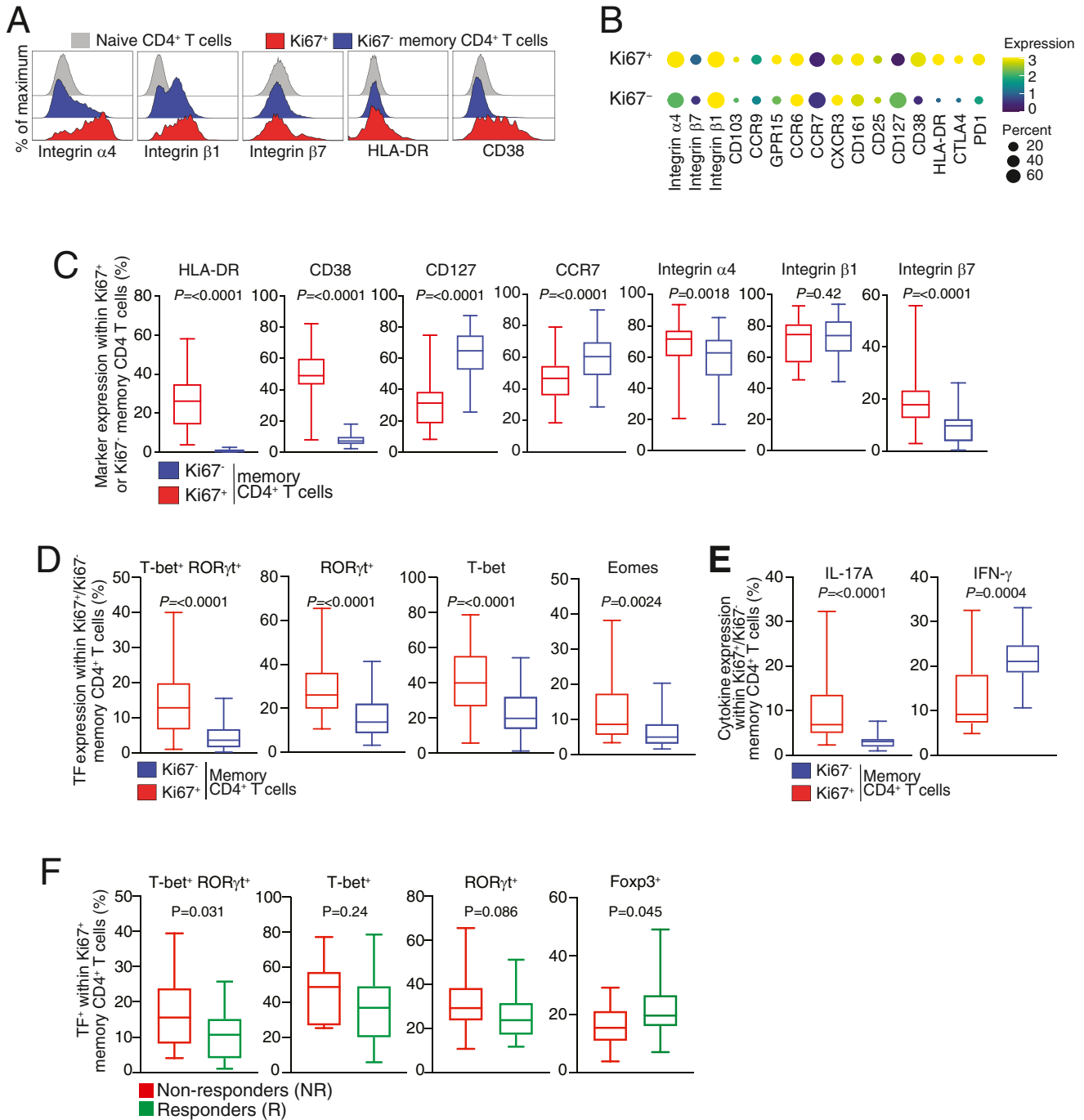


Figure 7. Distinctive features of proliferating effector CD4⁺ T cells in vedolizumab nonresponsive patients. (A) Histograms of FACS surface marker expression in a representative patient with IBD. Shown is the expression of the indicated markers on naïve, Ki67⁺, and Ki67⁻ memory CD4⁺ T cells. (B) Dot plot showing geomean expression of FACS surface markers on Ki67⁺ or Ki67⁻ memory CD4⁺ T cells in patients with IBD before therapy (n = 41). Expression normalized to naïve CD4⁺ T cells. (C) Percentage of indicated surface marker expression within Ki67⁺ and Ki67⁻ memory CD4⁺ T cells in patients with IBD. n = 29–44. Mann-Whitney test. (D) Percentage of indicated transcription factor expression within Ki67⁺ and Ki67⁻ memory CD4⁺ T cells in patients with IBD. n = 28–40. (E) Percentage of IL-17A and interferon (IFN)-gamma expression within Ki67⁺ and Ki67⁻ memory CD4⁺ T cells in patients with IBD. n = 20. (F) Expression of the indicated transcription factors within Ki67⁺ and Ki67⁻ memory CD4⁺ T cells in vedolizumab responders (R) vs nonresponders (NR). n = 18–32. Mann-Whitney test.

gluten-specific and *Salmonella*-specific circulating CD4⁺ T cells from patients with celiac disease³⁷ or healthy volunteers challenged with *Salmonella enterica*³⁸ showed a comparable phenotype to the cycling effector cells in patients with IBD.

This similarity suggests that the observed CD4⁺ T cells in patients with IBD, particularly vedolizumab nonresponders, could be cycling, activated microbiota-specific CD4⁺ T cells, which are known to be abundant in patients with IBD.³⁹

The observed circulating Ki67⁺ memory CD4⁺ T cells expressed homing receptors (CXCR3, CCR6, and GPR15) and adhesion molecules (integrins $\alpha4\beta1$ and $\alpha4\beta7$), which enable migration to the inflamed mucosal tissue.^{40,41} Indeed, a significant fraction of Ki67⁺ memory CD4 T cells expressed integrin $\alpha4\beta1$ and, to a lesser extent, integrin $\alpha4\beta7$, suggesting that they might not be sufficiently targeted by anti- $\alpha4\beta7$ integrin treatment. Integrin $\alpha4\beta1$ binds to VCAM-1 and integrin $\alpha4\beta7$ interacts with MadCAM-1, and both VCAM-1 and MadCAM-1 are up-regulated in the intestinal tissue of patients with IBD.^{42,43} However, vedolizumab does not influence the interaction between integrin $\alpha4\beta1$ and VCAM-1.¹² Initial efforts to target cell migration to intestinal tissue using a monoclonal antibody targeting $\alpha4$ integrin, natalizumab, which blocks both $\alpha4\beta1$ and $\alpha4\beta7$ integrins, significantly reduced intestinal inflammation, but at the cost of elevated risk of fatal progressive multifocal leukoencephalopathy.^{44–47} A small molecule oral integrin $\alpha4$ antagonist (AJM300) was well tolerated and induced a clinical response in patients with moderately active UC without increased risk of progressive multifocal leukoencephalopathy, which might be useful in patients with increased cycling circulating memory CD4⁺ T cells.⁴⁸ However, the pathogenic role of these cells and their mechanism of targeting remain unclear and need further investigation.

This study has several limitations. First, our sample size is small, comprising mostly patients with UC. Second, our study does not include the analysis of matched mucosal samples, limiting our understanding of the origin and characteristics of the observed increase in proliferating memory CD4⁺ T cells. Third, our novel findings of a predictive signature warrant additional investigations to elucidate underlying mechanisms. It is important to note that not all patients were profiled on all platforms, which may introduce bias or incomplete data representation. Nevertheless, our study expansively characterizes the circulating immune cell landscape using multimodal profiling, identifies alterations induced by vedolizumab treatment, and classifies therapy response. Validation of the predictive value of Ki67⁺ memory CD4⁺ T cells using a custom flow cytometry panel supported the robustness of our technical approach. However, a multicentric prospective study is needed to validate our signature in more heterogeneous patient populations. This will pave the way for developing a peripheral blood assay for precision therapy after validation in future multicentric studies.

Our study provides a comprehensive framework for assessing therapy response and understanding the mechanisms underlying resistance in chronic immune-mediated inflammatory diseases, such as IBD. Identifying personalized treatment strategies based on individual patient characteristics, as exemplified by our "stratify to target" approach, can significantly improve IBD management.

Supplementary Material

Note: To access the supplementary material accompanying this article, visit the online version of *Gastroenterology* at www.gastrojournal.org, and at <https://doi.org/10.1053/j.gastro.2024.09.021>.

References

1. Kaser A, Zeissig S, Blumberg RS. Inflammatory bowel disease. *Annu Rev Immunol* 2010;28:573–621.
2. Blumberg R, Powrie F. Microbiota, disease, and back to health: a metastable journey. *Sci Transl Med* 2012;4:137rv7.
3. de Souza HSP, Fiocchi C. Immunopathogenesis of IBD: current state of the art. *Nat Rev Gastroenterol Hepatol* 2016;13:13–27.
4. Khor B, Gardet A, Xavier RJ. Genetics and pathogenesis of inflammatory bowel disease. *Nature* 2011;474:307–317.
5. Zundler S, Becker E, Schulze LL, et al. Immune cell trafficking and retention in inflammatory bowel disease: mechanistic insights and therapeutic advances. *Gut* 2019;68:1688.
6. Neurath MF. Targeting immune cell circuits and trafficking in inflammatory bowel disease. *Nat Immunol* 2019;20:970–979.
7. Danese S, Vuitton L, Peyrin-Biroulet L. Biologic agents for IBD: practical insights. *Nat Rev Gastroenterol Hepatol* 2015;12:537–545.
8. Berlin C, Berg EL, Briskin MJ, et al. $\alpha4\beta7$ integrin mediates lymphocyte binding to the mucosal vascular addressin MAdCAM-1. *Cell* 1993;74:185–195.
9. Sandborn WJ, Feagan BG, Rutgeerts P, et al. Vedolizumab as induction and maintenance therapy for Crohn's disease. *N Engl J Med* 2013;369:711–721.
10. Feagan BG, Rutgeerts P, Sands BE, et al. Vedolizumab as induction and maintenance therapy for ulcerative colitis. *N Engl J Med* 2013;369:699–710.
11. Mehandru S, Colombel J-F, Juarez J, et al. Understanding the molecular mechanisms of anti-trafficking therapies and their clinical relevance in inflammatory bowel disease. *Mucosal Immunol* 2023;16:859–870.
12. Soler D, Chapman T, Yang L-L, et al. The binding specificity and selective antagonism of vedolizumab, an anti- $\alpha4\beta7$ integrin therapeutic antibody in development for inflammatory bowel diseases. *J Pharmacol Exp Ther* 2009;330:864–875.
13. Wyant T, Fedyk E, Abhyankar B. An overview of the mechanism of action of the monoclonal antibody vedolizumab. *J Crohns Colitis* 2016;10:1437–1444.
14. Fedyk ER, Wyant T, Yang L-L, et al. Exclusive antagonism of the $\alpha4\beta7$ integrin by vedolizumab confirms the gut-selectivity of this pathway in primates. *Inflamm Bowel Dis* 2012;18:2107–2119.
15. Calenda G, Keawvichit R, Arrode-Brusés G, et al. Integrin $\alpha4\beta7$ blockade preferentially impacts CCR6⁺ lymphocyte subsets in blood and mucosal tissues of naive rhesus macaques. *J Immunol* 2018;200:810–820.
16. Canales-Herrerias P, Uzzan M, Seki A, et al. Gut-associated lymphoid tissue attrition associates with response to anti- $\alpha4\beta7$ therapy in ulcerative colitis. *Sci Immunol* 2024;9:eadg7549.
17. Uzzan M, Tokuyama M, Rosenstein AK, et al. Anti- $\alpha4\beta7$ therapy targets lymphoid aggregates in the gastrointestinal tract of HIV-1-infected individuals. *Sci Transl Med* 2018;10:eaau4711.
18. Barré A, Colombel J-F, Ungaro R. Review article: predictors of response to vedolizumab and ustekinumab in

- inflammatory bowel disease. *Aliment Pharmacol Ther* 2018;47:896–905.
19. Colombel J-F, Narula N, Peyrin-Biroulet L. Management strategies to improve outcomes of patients with inflammatory bowel diseases. *Gastroenterology* 2017;152:351–361.e5.
 20. Atreya R, Neurath MF. Mechanisms of molecular resistance and predictors of response to biological therapy in inflammatory bowel disease. *Lancet Gastroenterol Hepatol* 2018;3:790–802.
 21. Digby-Bell JL, Atreya R, Monteleone G, et al. Interrogating host immunity to predict treatment response in inflammatory bowel disease. *Nat Rev Gastroenterol Hepatol* 2020;17:9–20.
 22. Bertani L, Caviglia GP, Antonioli L, et al. Serum interleukin-6 and -8 as predictors of response to vedolizumab in inflammatory bowel diseases. *J Clin Med* 2020;9:1323.
 23. Boden EK, Shows DM, Chiorean MV, et al. Identification of candidate biomarkers associated with response to vedolizumab in inflammatory bowel disease. *Digest Dis Sci* 2018;63:2419–2429.
 24. **Fuchs F, Schillinger D**, Atreya R, et al. Clinical response to vedolizumab in ulcerative colitis patients is associated with changes in integrin expression profiles. *Front Immunol* 2017;8:764.
 25. **Ananthakrishnan AN, Luo C**, Yajnik V, et al. Gut microbiome function predicts response to anti-integrin biologic therapy in inflammatory bowel diseases. *Cell Host Microbe* 2017;21:603–610.e3.
 26. Lee JWJ, Plichta D, Hogstrom L, et al. Multi-omics reveal microbial determinants impacting responses to biologic therapies in inflammatory bowel disease. *Cell Host Microbe* 2021;29:1294–1304.e4.
 27. Verstockt B, Verstockt S, Veny M, et al. Expression levels of 4 genes in colon tissue might be used to predict which patients will enter endoscopic remission after vedolizumab therapy for inflammatory bowel diseases. *Clin Gastroenterol Hepatol* 2020;18:1142–1151.e10.
 28. Osterman MT, Gordon IO, Davis EM, et al. Mucosal biomarker of innate immune activation predicts response to vedolizumab in Crohn's disease. *Inflamm Bowel Dis* 2019;26:1554–1561.
 29. **Shelton E, Allegretti JR**, Stevens B, et al. Efficacy of vedolizumab as induction therapy in refractory IBD patients. *Inflamm Bowel Dis* 2015;21:2879–2885.
 30. Dulai PS, Amiot A, Peyrin-Biroulet L, et al. A clinical decision support tool may help to optimise vedolizumab therapy in Crohn's disease. *Aliment Pharm Therap* 2020;51:553–564.
 31. **Hao Y, Hao S**, Andersen-Nissen E, et al. Integrated analysis of multimodal single-cell data. *Cell* 2021;184:3573–3587.e29.
 32. Morton AM, Sefik E, Upadhyay R, et al. Endoscopic photoconversion reveals unexpectedly broad leukocyte trafficking to and from the gut. *Proc Natl Acad Sci U S A* 2014;111:6696–6701.
 33. Zeissig S, Rosati E, Dowds CM, et al. Vedolizumab is associated with changes in innate rather than adaptive immunity in patients with inflammatory bowel disease. *Gut* 2019;68:25.
 34. Griseri T, McKenzie BS, Schiering C, et al. Dysregulated hematopoietic stem and progenitor cell activity promotes interleukin-23-driven chronic intestinal inflammation. *Immunity* 2012;37:1116–1129.
 35. **Griseri T, Arnold IC**, Pearson C, et al. Granulocyte macrophage colony-stimulating factor-activated eosinophils promote interleukin-23 driven chronic colitis. *Immunity* 2015;43:187–199.
 36. Funderburg NT, Park SRS, Sung HC, et al. Circulating CD4+ and CD8+ T cells are activated in inflammatory bowel disease and are associated with plasma markers of inflammation. *Immunology* 2013;140:87–97.
 37. Risnes LF, Reims HM, Doyle RM, et al. Gluten-free diet induces rapid changes in phenotype and survival properties of gluten-specific T cells in celiac disease. *Gastroenterology* 2024;167:250–263.
 38. Napolitani G, Kurupati P, Teng KWW, et al. Clonal analysis of *Salmonella*-specific effector T cells reveals serovar-specific and cross-reactive T cell responses. *Nat Immunol* 2018;19:742–754.
 39. **Hegazy AN, West NR**, Stubbington MJT, et al. Circulating and tissue-resident CD4+ T cells with reactivity to intestinal microbiota are abundant in healthy individuals and function is altered during inflammation. *Gastroenterology* 2017;153:1320–1337.e16.
 40. Moser B, Loetscher P. Lymphocyte traffic control by chemokines. *Nat Immunol* 2001;2:123–128.
 41. Habtezion A, Nguyen LP, Hadeiba H, et al. Leukocyte trafficking to the small intestine and colon. *Gastroenterology* 2016;150:340–354.
 42. Arihiro S, Ohtani H, Suzuki M, et al. Differential expression of mucosal addressin cell adhesion molecule-1 (MAdCAM-1) in ulcerative colitis and Crohn's disease. *Pathol Int* 2002;52:367–374.
 43. Jones SC, Banks RE, Haidar A, et al. Adhesion molecules in inflammatory bowel disease. *Gut* 1995;36:724.
 44. Sandborn WJ, Colombel JF, Enns R, et al. natalizumab induction and maintenance therapy for Crohn's disease. *N Engl J Med* 2005;353:1912–1925.
 45. Kleinschmidt-DeMasters BK, Tyler KL. Progressive multifocal leukoencephalopathy complicating treatment with natalizumab and interferon beta-1a for multiple sclerosis. *N Engl J Med* 2005;353:369–374.
 46. Langer-Gould A, Atlas SW, Green AJ, et al. Progressive multifocal leukoencephalopathy in a patient treated with natalizumab. *N Engl J Med* 2005;353:375–381.
 47. Gert VA, Marc VR, Raf S, et al. Progressive multifocal leukoencephalopathy after natalizumab therapy for Crohn's disease. *N Engl J Med* 2005;353:362–368.
 48. Matsuoka K, Watanabe M, Ohmori T, et al. AJM300 (carotegrast methyl), an oral antagonist of $\alpha 4$ -integrin, as induction therapy for patients with moderately active ulcerative colitis: a multicentre, randomised, double-blind, placebo-controlled, phase 3 study. *Lancet Gastroenterol Hepatol* 2022;7:648–657.

Author names in bold designate shared co-first authorship.

Received December 19, 2023. Accepted September 18, 2024.

Correspondence

Address correspondence to: Ahmed N. Hegazy, MD, PhD, Department of Gastroenterology, Infectious Diseases and Rheumatology, Charité-Universitätsmedizin Berlin, Campus Benjamin Franklin, Hindenburgdamm 30,

12203 Berlin, Germany or Deutsches Rheuma-Forschungszentrum, ein Institut der Leibniz-Gemeinschaft, 10117 Berlin, Germany. e-mail: ahmed.hegazy@charite.de or ahmed.hegazy@drfz.de; or Address correspondence for machine learning and statistical analysis to: Kevin Thurley, PhD, Deutsches Rheuma-Forschungszentrum, ein Institut der Leibniz-Gemeinschaft, Berlin, Germany; Institute of Experimental Oncology, Biomathematics Division, University Hospital Bonn, Bonn, Germany. e-mail: kevin.thurley@uni-bonn.de.

Acknowledgments

TRR241 IBDome Consortium: Imke Atreya,¹ Raja Atreya,¹ Petra Bacher,^{2,3} Christoph Becker,¹ Christian Bojarski,⁴ Nathalie Britzen-Laurent,¹ Caroline Bosch-Voskens,¹ Hyun-Dong Chang,⁵ Andreas Diefenbach,⁶ Claudia Günther,¹ Ahmed N. Hegazy,⁴ Kai Hildner,¹ Christoph S. N. Klose,⁶ Kristina Koop,¹ Susanne Krug,⁴ Anja A. Kühl,⁷ Moritz Leppkes,¹ Rocio López-Posadas,¹ Leif S.-H. Ludwig,^{8,9} Clemens Neufert,¹ Markus Neurath,¹ Jay Patankar,¹ Magdalena Prüb,³ Andreas Radbruch,⁵ Chiara Romagnani,³ Francesca Ronchi,⁶ Ashley Sanders,^{4,9} Alexander Scheffold,² Jörg-Dieter Schulzke,⁴ Michael Schumann,⁴ Sebastian Schürmann,¹ Britta Siegmund,⁴ Michael Stürzl,¹ Zlatko Trajanoski,¹⁰ Antigoni Triantafyllou,^{5,11} Maximilian Waldner,¹ Carl Weidinger,⁴ Stefan Wirtz,¹ and Sebastian Zundler¹; from the ¹Department of Medicine 1, Friedrich-Alexander University, Erlangen, Germany; ²Institute of Clinical Molecular Biology, Christian-Albrecht University of Kiel, Kiel, Germany; ³Institute of Immunology, Christian-Albrecht University of Kiel and University Hospital Schleswig-Holstein, Kiel, Germany; ⁴Charité-Universitätsmedizin Berlin, corporate member of Freie Universität Berlin and Humboldt-Universität zu Berlin, Department of Gastroenterology, Infectious Diseases and Rheumatology, Berlin, Germany; ⁵Deutsches Rheuma-Forschungszentrum, ein Institut der Leibniz-Gemeinschaft, Berlin, Germany; ⁶Charité-Universitätsmedizin Berlin, corporate member of Freie Universität Berlin and Humboldt-Universität zu Berlin, Institute of Microbiology, Infectious Diseases and Immunology, Berlin, Germany; ⁷Charité-Universitätsmedizin Berlin, corporate member of Freie Universität Berlin and Humboldt-Universität zu Berlin, iPATH.Berlin, Berlin, Germany; ⁸Berlin Institute of Health at Charité-Universitätsmedizin Berlin, Berlin, Germany; ⁹Max Delbrück Center for Molecular Medicine in the Helmholtz Association, Berlin Institute for Medical Systems Biology, Berlin, Germany; ¹⁰Biocenter, Institute of Bioinformatics, Medical University of Innsbruck, Innsbruck, Austria; and ¹¹Charité-Universitätsmedizin Berlin, corporate member of Freie Universität Berlin and Humboldt-Universität zu Berlin, Department of Rheumatology and Clinical Immunology, Berlin, Germany.

The authors thank Nadine Sommer and Anja A. Kühl for their support with sample collection within the IBDome consortium; J. Kirsch and T. Kaiser (Flow Cytometry Core Facility, DRFZ, Berlin) for technical assistance with cell sorting; Sarah Vitcetz and Gitta Heinz from the scRNAseq facility; Heike Hirsland and Sabine Baumgart for assistance with mass cytometry protocols, reagents, and acquisition (Mass Cytometry Group, DRFZ, Berlin); Yu-Hsien Hsieh for help with pilot experiments and analyses; and Ernesto Zarza Reyes for optimizing and revising the mass cytometry analysis code. The authors would like to express their gratitude to all the members of the Hegazy laboratory for their assistance with sample banking, as well as to our clinician and nurse colleagues in both the IBD inpatient and outpatient clinics.

Veronika Horn's current affiliation is Jill Roberts Institute for Research in Inflammatory Bowel Disease, Joan and Sanford I. Weill Department of Medicine, Division of Gastroenterology and Hepatology, Department of Microbiology and Immunology, Weill Cornell Medicine, Cornell University, New York, New York.

Credit Authorship Contributions

Veronika Horn, MD (Data curation: Equal; Formal analysis: Equal; Investigation: Equal; Methodology: Equal; Supervision: Supporting; Validation: Equal; Visualization: Equal; Writing – original draft: Lead; Writing – review & editing: Equal; Patient recruitment: Equal; Machine learning: Supporting; Single cell analysis: Supporting; Conceptualization: Supporting)

Camila A. Cancino, MSc (Conceptualization: Supporting; Formal analysis: Equal; Investigation: Equal; Methodology: Equal; Validation: Equal; Visualization: Equal; Data curation: Equal; Writing – review & editing: Supporting)

Lisa M. Steinheuer, PhD (Data curation: Equal; Formal analysis: Equal; Methodology: Equal; Visualization: Equal; Writing – review & editing: Supporting; Machine learning: Lead)

Benedikt Obermayer, PhD (Data curation: Equal; Formal analysis: Equal; Methodology: Equal; Visualization: Equal; Writing – review & editing: Supporting; Single cell analysis: Lead)

Konstantin Fritz, MD (Data curation: Supporting; Formal analysis: Supporting; Investigation: Supporting; Resources: Equal; Patient recruitment: Equal)

Anke L. Nguyen, MD, PhD (Resources: Supporting; Patient recruitment: Supporting)

Kim Susan Juhran (Resources: Supporting)

Christina Plattner, PhD (Data analysis: Supporting)
 Diana Bösel, RA (Investigation: Supporting)
 Lotte Oldenburg, MD (Resources: Supporting)
 Marie Burns, PhD (Methodology: Supporting; Resources: Supporting)
 Axel Ronald Schulz, PhD (Methodology: Supporting; Resources: Supporting)
 Mariia Saliutina, MSc (Investigation: Supporting)
 Eleni Mantzivi, MD (Resources: Supporting)
 Donata Lissner, MD (Resources: Supporting)
 Thomas Conrad, PhD (Resources: Supporting)
 Mir-Farzin Mashreghi, PhD (Resources: Supporting)
 Sebastian Zundler, MD (Resources: Supporting)
 Elena Sonnenberg, MD (Resources: Supporting)
 Michael Schumann, MD (Resources: Supporting)
 Lea-Maxie Haag, MD (Resources: Supporting)
 Dieter Beule, PhD (Resources: Supporting)
 Lukas Flatz, MD (Resources: Supporting)
 TRR241 IBDome Consortium (Resources: Supporting)
 Zlatko Trajanoski, PhD (Resources: Supporting)
 Geert D'Haens, MD (Resources: Supporting)
 Carl Weidinger, MD (Resources: Supporting)
 Henrik E. Mei, PhD (Resources: Supporting; Methodology: Supporting)
 Britta Siegmund, MD (Project administration: Supporting; Supervision: Supporting; Resources: Supporting)
 Kevin Thurley, PhD (Supervision: Supporting; Project administration: Supporting; Writing – review & editing: Supporting; Formal analysis: Lead)
 Ahmed N. Hegazy, MD, PhD (Supervision: Lead; Project administration: Lead; Funding acquisition: Lead; Conceptualization: Lead; Methodology: Supporting; Writing – original draft: Lead; Writing – review & editing: Lead)

Conflicts of interest

These authors disclose the following: Britta Siegmund received lecture fees from Abbvie, BMS, CED Service GmbH, Chiesi, Falk, Forga Software, Galapagos, IBD Passport, Janssen, Materia Prima, Pfizer, and Lilly; consulting fees from Abbvie, Arena Pharma, Boehringer, BMS, Celgene, CT-Scout, Endpoint Health, Galpagos, Gilead, Janssen, Landos, Lilly, Pfizer, PredictImmune, and PsiCro; and research support from Pfizer (all payments went to institution). Geert D'Haens has received research grants from Abbvie, Alimentiv, BMS Eli Lilly, J&J, Pfizer, and Takeda; consulting fees from Abbvie, Agomab, Alimentiv, AstraZeneca, AM Pharma, AMT, Arena Pharmaceuticals, Bristol-Myers Squibb, Boehringer Ingelheim, Celltrion, Eli Lilly, Exeliom Biosciences, Exo Biologics, Galapagos, Index Pharmaceuticals, Kaleido, Roche, Gilead, GlaxoSmithKline, Gossamerbio, Pfizer, Immunic, Johnson & Johnson, Origo, Polpharma, Procidia Diagnostics, Prometheus Laboratories, Prometheus Biosciences, Progenity, and Protagonist; speaking fees from Abbvie, Arena, BMS, Boehringer Ingelheim, Celltrion, Eli Lilly, Galapagos, Gilead, Pfizer, and Takeda; and is on the data monitoring board: Galapagos, AstraZeneca, and Seres Health. The remaining authors disclose no conflicts.

Funding

Ahmed N. Hegazy is supported by a Lichtenberg fellowship (Az: 92 087) and a "Corona Crisis and Beyond" grant by the Volkswagen Foundation, a BIH Clinician Scientist grant and German Research Foundation 375876048-DFG-TRR241-A05 and INST 335/597-1, as well as by the ERC-StG "iMOTIONS" grant (101078069). This project was funded by a BIH Cohort Sequencing Program grant provided to Ahmed N. Hegazy. Veronika Horn received a Gerok fellowship from the German Research Foundation DFG-TRR241 and is supported by a Walter Benjamin fellowship from the German Research Foundation (HO 7399/1-1). Anke L. Nguyen was supported by the Research Training Program Stipend (Monash University). Henrik Mei received funding from the state of Berlin and from the DFG, projects ME3644/5-1 and ME3644/11-1. Kevin Thurley was supported by Germany's Excellence Strategy grants EXC2151-390685813 and EXC2047-390873048. Carl Weidinger was supported by the German Research Foundation CRC-TRR241-A09, CRC-TRR241-B01 (INST 335/597-1), WE5303/3-1, as well as by the Fritz-Thyssen Foundation. Mir Farzin Mashreghi received funding from the state of Berlin and the "European Regional Development Fund" (ERDF 2014-2021, EFRE 1.8/11, Deutsches Rheuma-Forschungszentrum), the Leibniz Association (Leibniz Collaborative Excellence, TargArt and ImpACT), and the German Federal Ministry of Education and Research (BMBF) projects CONAN and TreAT, Leibniz Association (Leibniz Collaborative Excellence, TargArt and ImpACT), and the German Federal Ministry of Education and Research (BMBF, CONAN, TreAT, 01GL2401C). Britta Siegmund was supported by the German Research Foundation CRC-TRR241 (project-ID: 375876048), CRC1340 (project-ID: 372486779), CRC1449 (project-ID: 321232613), and INST 335/597-1.

Data Availability

The data, analytical methods, and study materials will be made available to other researchers upon publication. Please refer to the Materials and Methods section for details.